

LAYERED COMPOUNDS BASED ON PERFORATED GRAPHENE

N. F. Yudanov,¹ A. V. Okotrub,^{1,2} L. G. Bulusheva,^{1,2}
I. P. Asanov,^{1,2} Yu. V. Shubin,¹ L. I. Yudanova,¹
N. I. Alferova,¹ V. V. Sokolov,¹ N. N. Gavrilov,¹
and V. A. Tur¹

UDC 546.26-162:546.16:546.162

A method to obtain previously unknown layered structure composed of stacks of perforated graphene sheets is developed. The method consists in the thermal decomposition of graphite oxide in the concentrated H₂SO₄ and H₃PO₄ medium. In order to confirm the presence of holes in graphene layers, a large set of chemical and physicochemical analysis methods are applied. Based on a new matrix, treated thermally and chemically, layered compounds are obtained: oxide, fluoride, and fluoroxide of two types. The obtained compounds are analyzed by transmission electron microscopy, infrared absorption spectroscopy, Raman spectroscopy, X-ray photoelectron spectroscopy, thermogravimetric analysis, and powder X-ray diffraction.

Keywords: graphite, layered compounds, perforated graphene, carbon fluoride.

INTRODUCTION

Layered structures are of considerable interest both because of their physical properties and a matrix to obtain various chemical compounds. Thus, based on the graphite structure a considerable number of diverse compounds have been synthesized. Numerous papers describe the synthesis of these compounds. They can be divided into two main trends: 1) synthesis of intercalation graphite compounds and 2) graphite modification by the covalent addition of fluorine, oxygen, and chlorine atoms to carbon networks. Modified graphite in turn can be used to obtain intercalates. Information on graphite and its compounds is concentrated in the monograph [1]. Both trends have a common feature: maintenance of the integrity of carbon graphite networks (graphene).

In this work, we propose a method to obtain a new layered carbon structure by generating many defects in the form of holes in the carbon networks of graphite with maintaining the network packing character. The holes cause a substantial increase in the number of carbon atoms bonded only to two neighbors and therefore exhibiting chemical properties different from those of *sp*²-hybridized atoms. The properties of such a structure remarkably differ from the properties of graphite in both physical parameters (density, conductivity) and reactivity. Apart from the available possibility of producing various layered compounds with new properties based on the new structure, this structure can be of interest as a source of perforated graphene sheets. Now we can see a spurt of interest in isolated graphite layers (graphene, especially graphene containing diverse defects); in particular, the properties of perforated graphene are being studied [2, 3]. The interest in these objects is due to the possibility of a target change in their properties by adding functional groups to carbon atoms around the hole

¹A. V. Nikolaev Institute of Inorganic Chemistry, Siberian Division, Russian Academy of Sciences, Novosibirsk; spectrum@niic.nscc.ru. ²Novosibirsk State Technical University. Translated from *Zhurnal Strukturnoi Khimii*, Vol. 52, No. 5, pp. 932-938, September-October, 2011. Original article submitted February 11, 2011.

perimeters. This expands the application possibilities of graphene in diverse fields. Chemical compounds obtained based on the new structure can become a source of functionalized monolayers of perforated graphene.

As a solution method for the posed problem the decomposition of graphite oxide under mild conditions was used. Heating of graphite oxide to a temperature of ~200°C is known to cause its rapid decomposition with a flash and the formation of fine carbon; at the same time, part of carbon atoms is removed in the form of CO and CO₂ [1]. Removal of a part of atoms from graphite networks should inevitably result in the formation of holes in them; however, a vigorous gas evolution leads to the rupture of layers. In order to maintain the integrity of layers it is required to permit a free gas evolution from interlayer spaces. This is possible only when the decomposition proceeds sufficiently slowly. Under these conditions gas molecules have time to leave the interlayer spaces due to diffusion. Since the decomposition of graphite oxide is an exothermal process, to decrease its rate it is necessary to continuously and efficiently remove the released heat energy. In this work, H₂SO₄ or H₃PO₄ molecules, which can be easily introduced into the interlayer spaces of graphite oxide because of its ability to yield intercalation compounds with concentrated acids, were used as a heatsink. Apart from the role of a heatsink, acid molecules cause an increase in the interlayer distance in graphite oxide, which also permits a steady behavior of the process, facilitating the evolution of gases from interlayer spaces.

EXPERIMENTAL. RESULTS AND DISCUSSION

The samples were analyzed by high-resolution transmission electron microscopy (TEM) on a JEM-2010 (JEOL, Japan) electron microscope with an accelerating voltage of 200 kV and a lattice resolution of 1.4 Å. X-ray photoelectron spectra (XPS) were obtained on a PHOIBOS 150 (Specs) spectrometer. The spectra were excited by monochromated AlK_α radiation and measured at the electron analyzer transmission energy of 20 eV. IR spectra were recorded on a Scimitar FTS 2000 Fourier spectrometer; samples for the measurement were prepared by pressing in pellets with KBr. Thermal properties were investigated on a C derivatograph (MOM, Hungary). Heating was performed in a He flow (analytical grade) with a rate of 2 deg/min. X-ray diffraction was performed using a DRON 3M diffractometer. Raman spectra were measured on a Triplemate (SPEX model) spectrometer equipped with a multichannel detector at photon excitation with the wavelength $\lambda = 488$ nm.

In this work, we used graphite oxide samples obtained by graphite oxidation with a CrO₃ solution in anhydrous HF [4]. The IR spectrum is depicted in Fig. 2a; the diffraction pattern is presented in Fig. 3a.

Graphite oxide was decomposed as follows. A weighed amount of the compound (~1 g) was poured in a beaker with 100 ml of concentrated H₂SO₄. The mixture was kept for 10 min at room temperature. The color of graphite oxide changed from yellow to green. Then the mixture was heated until H₂SO₄ vapor evolved. From this moment the heating lasted for 10 min, 20 min, and 60 min in three series of experiments. After cooling the reaction mixture to room temperature, it was poured into a beaker with 500 ml of distilled water. The obtained black products (**I**) were filtered off on a glass filter and washed to a neutral reaction of washing waters. Without drying the products were washed on a filter with a small amount of a concentrated NH₃ solution, and then again with water to remove low molecular oxidation products that color the filtrate brown. Finally, the products were air-dried at room temperature.

TEM images of **I** (Fig. 1a and b) show that the obtained products retained the layered structure of the particles, and their surface looks rough. Since we failed to obtain a good image of the monolayer, we carried out a computer simulation of the image in Fig. 1b. By means of a graphic editor we composed 6 different images of the type shown in Fig. 1c with a random arrangement of white spots simulating holes in the carbon network. We set the image transparency to 90% and then imposed them on each other. The resulting image after the achievement of appropriate brightness and contrast is shown in Fig. 1d, and its reduced image is given in Fig. 1b. A similarity between the model and experimental images is observed.

The XPS spectra of **I** show the contributions of carbon and oxygen atoms. The surface concentration of oxygen atoms is 17 at.%. In the C1s spectra, it is possible to distinguish a main asymmetric peak at 284.6 eV, which corresponds

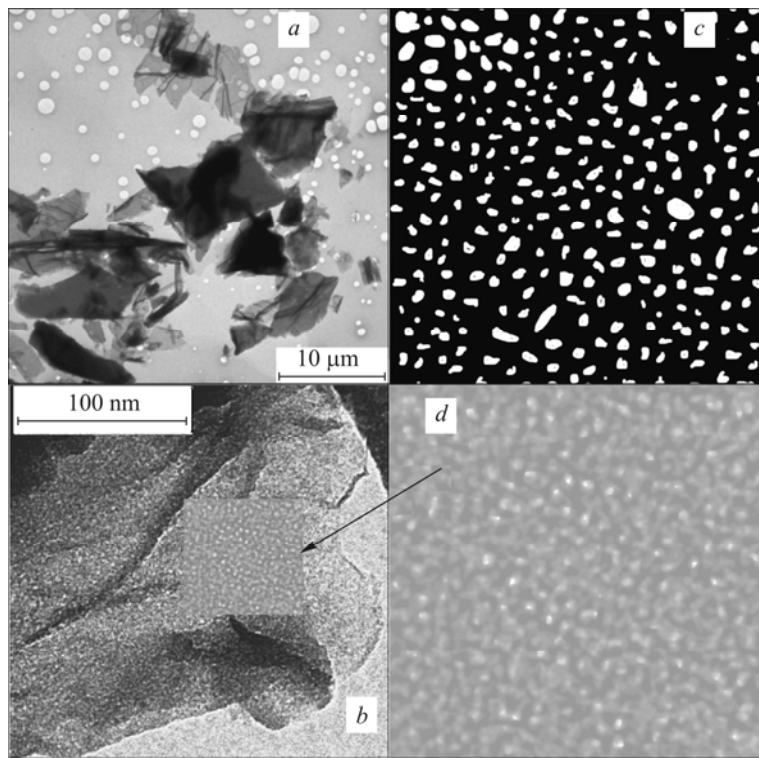


Fig. 1. TEM images of perforated graphite oxide (*a* and *b*); stages of the TEM image simulation using a graphic editor (*c* and *d*).

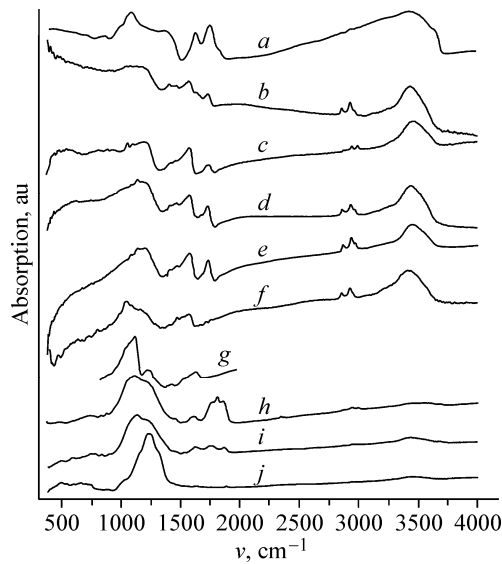


Fig. 2. IR spectra: initial graphite oxide (*a*), decomposition product of graphite oxide in H_3PO_4 (*b*), decomposition products of graphite oxide in H_2SO_4 (heating time in H_2SO_4 of 10 min, 20 min, and 60 min) (*c*, *d*, and *e*), calcinations product of perforated graphite oxide (*f*), fragment of the spectrum of C_2F (*g*), BrF_3 fluorination product of perforated graphite oxide (*h*), BrF_3 fluorination product of calcined perforated graphite oxide (*i*), F_2 fluorination product of perforated graphite oxide (*j*).

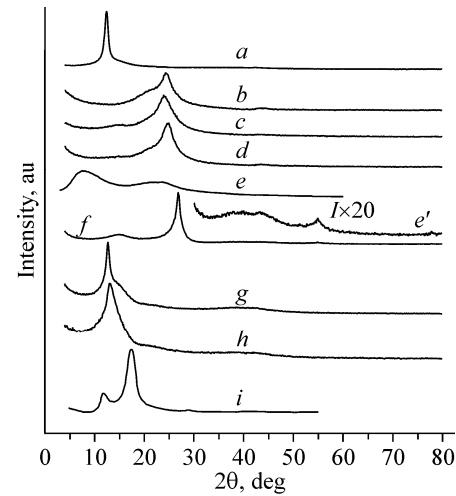


Fig. 3. Diffraction patterns: initial graphite oxide (*a*), decomposition products of graphite oxide in H_2SO_4 (heating time in H_2SO_4 of 10 min, 20 min, and 60 min) (*b*, *c*, and *d*), wet perforated graphite oxide (*e*), calcined perforated graphite oxide (*f* and *f'*), BrF_3 fluorination product of perforated graphite oxide (*g*), BrF_3 fluorination product of calcined perforated graphite oxide (*h*), graphite fluorination product (*i*).

to carbon atoms in the graphite matrix, and less intense components at 286.2 eV and 288.5 eV respectively. The O1s spectrum exhibits two intense components at 531.4 eV and 533.2 eV with approximately equal intensity, which correspond to oxygen atoms of carboxyl and hydroxyl groups [5, 6] respectively, and also a weak line at 535.9 eV that corresponds to water molecules.

The IR spectra of **I** obtained in three series of experiments (heating time in acid 10 min, 20 min, and 60 min) are presented in Fig. 2c-e respectively. First of all, the presence of absorption bands at 2854 cm^{-1} and 2925 cm^{-1} should be noted, which unambiguously evidence the presence of C–H bonds (2854 cm^{-1} and 2924 cm^{-1} in *n*-heptane). It is possible to assume the formation of C–H bonds to be due to the appearance of radical centers on carbon atoms during the destruction of graphite oxide. Then hydrogen atoms join these centers. Apart from the mentioned bands, the absorption band at 1725 cm^{-1} can be assigned to C=O bonds with enough confidence. A broad band with the maximum at 3450 cm^{-1} belongs to the stretching vibrations of O–H groups of both water molecules and those bonded to the carbon lattice. The absorption band at 1569 cm^{-1} can be assigned to the bending vibrations of O–H groups bonded to carbon. Our attention is engaged by a decrease in the absorption intensity in the range from 900 cm^{-1} to 380 cm^{-1} as the heating time of graphite oxide in H_2SO_4 increases. It was suggested that this effect related to partial etching of **I** with hot H_2SO_4 because it has strong oxidizing properties. In order to check this assumption, the decomposition reaction of graphite oxide was conducted in the concentrated H_3PO_4 medium, which does not have oxidizing properties. As seen from the IR spectrum of the obtained product (Fig. 2b), an increase in the absorption intensity is observed instead of a dip in the low-frequency region of the spectrum. In the 900 – 4000 cm^{-1} range, the absorption bands of **I** and the product obtained in the H_3PO_4 medium completely coincide, which indicates their identical nature. This experiment evidences in favor of the assumption made. Moreover, after washing the obtained product with an NH_3 solution the filtrate is not colored, as noted in the description of the synthesis of **I**. This can be observed when colored low molecular substances form during partial oxidation of **I** with hot H_2SO_4 . The nature of the low-frequency dip in the IR spectra of **I** remains unclear, especially because this dip is absent in the IR spectra of fluoro derivatives of **I**, as shown below.

Diffraction patterns of **I**, which dramatically differ from the diffraction patterns of graphite oxide (Fig. 3a), are depicted in Fig. 3b-e. Broad non-integer maxima of the $00l$ type are observed, which may indicate defects in the parallel packing of carbon layers induced by the presence of oxygen-containing groups protruding above the carbon network. Positions of the most intense maxima in the diffraction patterns b-e correspond to the d/n values of 3.6 \AA , 3.7 \AA , and 3.6 \AA respectively. The 100 reflections for all samples are much broadened and have extremely low intensity. The reason of this, as can be assumed, is a quite perfect texture of the samples and a very small CSR size of the carbon network. The latter does not contradict to the assumption of the perforation of graphene layers. It should be noted that the unambiguous dependence of the diffraction pattern character on the time of sample heating in H_2SO_4 is not established, whereas in the IR spectra, this dependence is clearly traced. Minor differences in the diffraction patterns, as could be expected, are due to the hydrophilicity of oxygen-containing groups bonded to the carbon network and the penetration of water molecules from the air whose humidity was not controlled during the measurements. In order to determine the effect of H_2O molecules penetrated into the interstitial spaces of **I**, we measured a wet sample of **I** after keeping it in water for 3 days. The diffraction pattern is presented in Fig. 3e. This diffraction pattern drastically differs (the positions of much broadened maxima correspond to the d/n values of 11.0 \AA , 4.11 \AA , and 3.8 \AA) from the diffraction patterns of the air-dried samples of **I**. The obtained result does not contradict to the made assumption, and moreover, indicates the ability of **I** to absorb H_2O , which results in even stronger distortions of carbon layers than those in **I**.

The Raman spectra of **I** measured in the 1000 – 2300 cm^{-1} range contain two maxima at 1360 cm^{-1} and 1596 cm^{-1} that correspond to *D* and *G* modes of the graphite network. A calculation performed by the formula $L_a = (2.4 \cdot 10^{-10}) \cdot \lambda_{\text{laser}}^4 \cdot (D/G)^{-1}$ [7, 8] (where L_a is the length of the defect-free region of the graphite lattice (nm); λ is the laser radiation wavelength (nm); *D* and *G* are the areas of the corresponding maxima) yields a value of 8.5 nm for all three samples of **I**. This means that the average distance between the holes in the carbon network does not depend (within the accuracy of this method) on the heating time of **I** in H_2SO_4 .

In the DTA curve obtained on decomposition of **I** in the He flow at a heating rate of 2 deg/min, three endoeffects with maximum positions at 123°C, 280°C, and 458°C are observed. It should be noted that initial graphite oxide decomposes with an exoeffect. The weight loss curve (TG) has no pronounced maxima, but at 620°C there is a crisis, after which the linear temperature dependence of the weight loss is observed up to the maximum measurement temperature of 900°C. The total weight loss for the sample of **I** heated in H₂SO₄ for 20 min is 21.3 wt.%. It is interesting that the TG curve still does not flatten at 900°C. In order to explain this fact additional studies are required.

The IR spectrum of the sample of **I** heated to 700°C and then cooled to room temperature in the N₂ flow is depicted in Fig. 2f. An almost complete absence of the absorption band at 1725 cm⁻¹ is noted, which is characteristic of the C=O bond vibrations. This evidences the removal of both carbonyl and carboxyl groups during thermal treatment. At the same time, the absorption bands corresponding to the C–H bonds are retained. The reason for this can be both the retention of C–H bonds during thermal treatment and the addition of H₂O molecules to active centers of the carbon network with the formation of C–H and C–OH bonds during air-storage of the sample. The latter assumption seems to be more probable because according to the XPS data, this compound contains 6 at.% of oxygen, especially because the retention of C–O bonds at 700°C causes doubts.

In order to measure the electric conductivity, pellets with a density of 2.11 g/cm³ and 1.67 g/cm³ respectively were pressed from purified natural graphite and **I** under the same conditions. The ρ values found for them are 109 1/Ohm·m and 66 1/Ohm·m. Consequently, the electric conductivity of **I** is less than two times lower than the electric conductivity of graphite, while graphite oxide is a dielectric.

The set of obtained results allows us to state that compound **I** is a derivative of the structure consisting of perforated graphene stacks. Since this compound does not have an accepted nomenclature name, we propose to call it perforated graphite oxide (PGO) for convenience. This name emphasizes its relationship with graphite, whereas the occurrence of a few types of oxygen atom addition to carbon lattice atoms does not contradict to the use of the term “oxide,” taking into account that graphite oxide also contains different types of oxygen–carbon bonds. It should be added that the attempt to oxidize PGO more fully with a KMnO₄ solution in concentrated H₂SO₄ results in a nearly complete dissolution of the product with the formation of a red-brown solution. Under these conditions, graphite reacts with the formation of graphite oxide.

In order to better understand the properties of PGO and the product of its calcination in the N₂ atmosphere, they were treated with fluorinating reagents: BrF₃ and F₂. Fluorination with BrF₃ was performed as follows. A weighed amount of PGO or its calcined product (~0.5 g) in a perforated Teflon sample bottle was placed into saturated Br₂ vapors for 1 day. Then the sample bottle was put into a Teflon reactor over the BrF₃ and Br₂ solution in the 1/1 weight ratio. Having kept the sample bottle in the reactor for 5–30 days, it was taken out and held in a dry N₂ flow to a constant weight of the obtained product. For the fluorination of PGO with F₂ a weighed amount of PGO in a nickel boat was placed in a nickel tube reactor with a heater. After heating the reactor to 200–220°C the F₂ flow was fed into it from an electrolyzer (KF·2HF electrolyte, electrolyte temperature 100°C) without purifying the gas from HF.

The PGO fluoro derivative (**II**) obtained by fluorination with BrF₃ represents transparent light yellow plates resembling graphite oxide and also having dielectric properties. Fig. 2g depicts a fragment of the IR spectrum of the intercalate obtained by graphite fluorination in vapors over a BrF₃ solution in Br₂, which contains only absorption bands of the C₂F_x matrix. A comparison of this fragment with the IR spectrum of **II** shows that they are substantially different. If the IR spectrum of C₂F_x contains a well-resolved doublet with maximum positions at 1114 cm⁻¹ and 1225 cm⁻¹, then in the spectrum of **II**, the doublet is not resolved. The reason for this can be both an increase in the 1225 cm⁻¹ band intensity and the appearance of a new band between the doublet bands. Moreover, the spectrum of **II** exhibits a 1680–1928 cm⁻¹ broad band that is absent in the spectrum of C₂F_x. It is difficult to assign this band to any bonds; it is only possible to suppose that it is due to the presence of oxygen in the composition of the fluoro derivative. According to the XPS data, the composition of **II** contains 13 at.% of oxygen. The diffraction pattern of **II** (Fig. 3g) also drastically differs from the product of graphite fluorination under the same conditions (Fig. 3*i*). Based on the above, it is possible to conclude that **II** is perforated graphite fluoroxide.

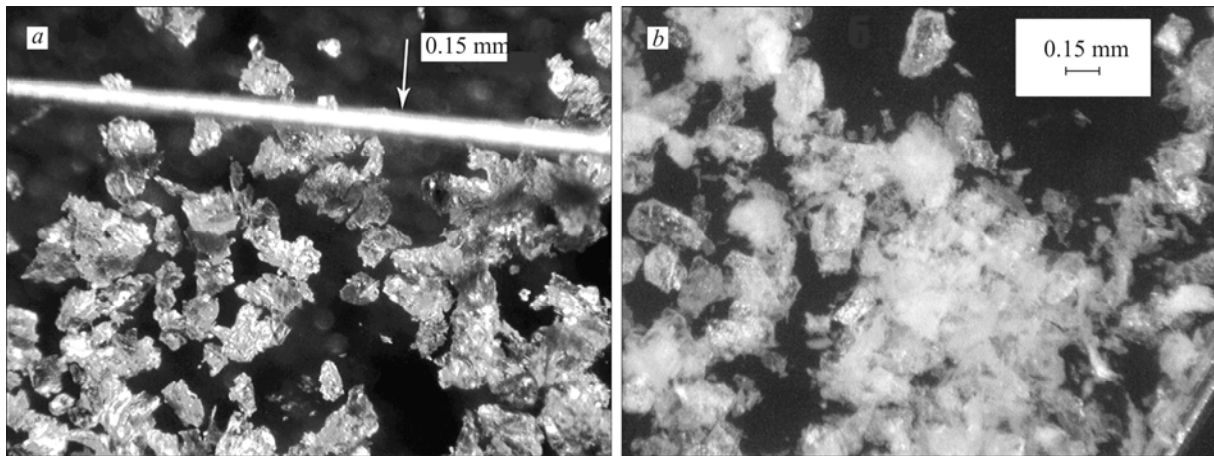


Fig. 4. Photographs of initial graphite oxide (*a*) and F_2 fluorination product of perforated graphite oxide (*b*).

A fluoro derivative of the PGO calcined product (**III**), also obtained by BrF_3 fluorination, represents transparent yellow-brown plates. Such a color can be due to that small regions of the carbon network are inaccessible for BrF_3 molecules. The reason for this can be the formation of a few interlayer C–C bonds during the thermolysis of PGO. This layer bonding should also hinder their glide due to shear stress. This assumption is consistent with the fact that calcined PGO, unlike graphite and PGO, is poorly pressed in pellets. In the IR spectrum of **III** (Fig. 2*i*), absorption in the $800\text{--}1500\text{ cm}^{-1}$ range is similar to absorption in the spectrum of **II**. The difference is seen in that the spectrum of **III** lacks the broad band at $1680\text{--}1928\text{ cm}^{-1}$ that is due, as is supposed in the discussion of the spectrum of **II**, to the presence of carbon lattice bonds with oxygen atoms. According to the XPS data, the concentration of oxygen atoms on the sample surface decreased below 5 at.%, which agrees with the IR data. The diffraction patterns of **III** and **II** are similar, but the positions of maxima (2θ , deg) are somewhat different: 12.7 ($d/n = 6.97\text{ \AA}$) and 13.1 ($d/n = 6.75\text{ \AA}$) respectively.

The product of PGO fluorination with F_2 (**IV**) represents transparent colorless plates. Fig. 4*a* and *b* presents the photographs of graphite oxide used to obtain PGO and **IV** respectively. The IR spectrum of **IV** exhibits an absorption band with the maximum at 1224 cm^{-1} . The occurrence of this band is caused by C–F bonds and is characteristic of the products of high temperature fluorination of carbon materials and graphite [9]. On the contour of the observed band there are two shoulders from both the side of smaller ν values (relative to the maximum position) and the side of larger values. This indicates the presence of three different types of C–F bond in **IV**. Indeed, according to the XPS data, the C1s spectrum has three main components related to CF, C–F₂, and C–F₃ groups. The composition of **IV** determined from the ratio of C1s components corresponds to the formula $CF_{1.32}$, which practically coincides with the composition of the most fluorinated fluorides of graphite-like materials: $CF_{1.33}$ [9]. It is essential to note that graphite fluorination with F_2 at 600°C yields a compound of the composition $(CF)_n$.

The results allow us to state that PGO as well as the compounds obtained from it by thermal and chemical treatment are the derivatives of the structure composed of perforated graphene layers. There are reasons to think that this structure can be used to synthesize layered compounds with very diverse properties.

In conclusion, to explain the causes of the dip in the low-frequency region of the IR absorption spectra of PGO it is possible to make the following assumption. Recent studies of the properties of metal films with nanohole lattices made in them by a focused ion beam have revealed a few interesting physical effects. In particular, it is shown that during electromagnetic irradiation of perforated metal films in the wavelength range of 200 nm to 2000 nm, a dramatic increase in incident radiation transmission is observed at some λ values [10]. The authors explain this effect by the interaction of surface plasmons, excited by incident electromagnetic radiation, with the perforated metal film. Since in the case of PGO we deal with perforated conductive films (perforated graphene), it is possible to assume that the observed dip is related to a similar

mechanism. The occurrence of polar C=O bonds at carbon atoms around the hole perimeters is likely to play an important role in this mechanism.

CONCLUSIONS

The thermal decomposition of graphite oxide in the medium of concentrated H₂SO₄ and H₃PO₄ results in the formation of oxygen- and hydrogen-containing derivatives of a new carbon structure. This structure consists of perforated graphene layers arranged in parallel to each other. The average distance between the edges of holes along the carbon planes is 8.5 nm. Based on the new carbon structure, we obtained layered compounds with the properties drastically different from the properties of layered graphite compounds close in composition. The results of the work demonstrate a possibility to produce a new class of layered compounds based on the structure composed of perforated graphene layers.

The work was supported by the Ministry of Education and Science of the Russian Federation, grant 2.1.2./9444.

REFERENCES

1. A. R. Ubbelohde and F. A. Lewis, *Graphite and Its Crystal Compounds*, Oxford University Press, Oxford, UK (1960).
2. Jiang De-en, V. R. Cooper, and Sh. Dai, *Nano Lett.*, **9**, No. 12, 4019-4024 (2009).
3. S. Blankenburg, M. Bieri, R. Fasel, et al., *Small.*, **6**, No. 20, 2266-2271 (2010).
4. N. F. Yudanov, A. S. Nazarov, and V. V. Lisitsa, *Zh. Neorg. Khim.*, **21**, 2273-2276 (1976).
5. U. Zielke, K. J. Hüttinger, and W. P. Hoffman, *Carbon*, **34**, 993-998 (1996).
6. D. Yang, A. Velamakanni, G. Bozoklu, et al., *Carbon*, **47**, 145-152 (2009).
7. M. S. Dresselhaus, A. Jorio, A. G. Sousa Filho, and R. Saito, *Phil. Trans. R. Soc. A*, **368**, 5355-5377 (2010).
8. M. A. Pimenta, G. Dresselhaus, M. S. Dresselhaus, et al., *Phys. Chem. Chem. Phys.*, **9**, 1276-1291 (2007).
9. V. N. Mit'kin, *J. Struct. Chem.*, **44**, No. 1, 82-115 (2003).
10. T. W. Ebbesen, H. J. Lezec, H. F. Ghaemi, et al., *Nature*, No. 391, 667-669 (1998).